Interfacial Layer between a Mercury Electrode and Dilute Aqueous Solutions of Alkali-Metal Chloride at Potentials of the Cathodic Limiting Current Plateau

Katsuo TAKAHASHI and Reita TAMAMUSHI

The Institute of Physical and Chemical Research, Hirosawa, Wako, Saitama 351

(Received June 27, 1975)

The electrochemical properties of the interfacial layer between a DME and dilute aqueous solutions of MCl (M: alkali-metal) at the cathodic limiting current plateau were studied by means of impedance measurements at relatively low frequencies ($\leq$250 Hz). From the frequency and potential dependence of the capacitive and the resistive components of the electrode impedance, the following conclusions were obtained concerning the properties of the interfacial layer under the above condition: (i) when the concentration of cations is extremely low in the vicinity of the electrode surface, the impedance behaves as if the conventional double-layer were absent: (ii) the impedance behavior of the present system can be explained by assuming an equivalent circuit which is given by a series combination of the Warburg impedance for the reduction of M^+ and the resistance of solution; and (iii) such an interfacial layer is conventionally called "the Nernst double-layer" and its formation is determined by the mass-transport of the reacting species M^+.

A conventional double-layer of the Helmholtz-Gouy-Chapman type is formed at a polarizable electrode/solution interface by some nonfaradaic interaction between the electrode and ionic species in the solution. The structure of such a double-layer has been extensively studied.[1,2] However, only a limited amount of information is available on the properties of an electrode/solution interface where the concentration of electrochemically-inactive ions is extremely low.[3-5]

The capacitance behavior of the interface between mercury and dilute electrolyte solutions was reported in previous papers.[6,7] Contrary to Grahame's model of the double-layer, the capacitance of a compact double-layer at highly negative electrode potentials was found to decrease with a decrease in the concentration of electrolytes.[6] It was observed that the capacitance of a dropping mercury electrode (DME)/TlOH system decreased markedly at electrode potentials in the region of the cathodic limiting current plateau.[7] Such a decrease in the double-layer capacitance was explained in terms of the deficiency of electrochemically-inactive cations forming the conventional double-layer.

This study deals with the impedance behavior of a DME/MCl (M: alkali-metal) system in the potential region of the cathodic limiting-current plateau. Sluyters-Rehbach *et al.*[8,9] measured the impedance of similar systems and discussed the electrode reaction of alkali-metal cations at a DME; in contrast to their study, our measurements were carried out with dilute aqueous solutions (less than a few mM) of alkali-metal chlorides in order to obtain detailed information on the structure of the interfacial layer where the concentration of cations is extremely low. From the frequency dependence of the electrode impedance, a possible equivalent circuit is proposed, and the characteristics of such an interfacial layer are discussed.

Experimental

The conductive and the susceptive components of the admittance of an electrode/solution system were measured as a function of the electrode potential by means of a phase-sensitive AC polarograph consisting of a conventional AC polarographic unit and two phase-sensitive detectors. In order to make accurate measurements with high-impedance systems, the phase-sensitive detectors were carefully adjusted and calibrated by using appropriate dummy-cells of known resistors and capacitors. The details of the measuring circuits and procedures have been reported elsewhare.[10]

The cell employed was a glass beaker of 100 cm^3 capacity with a silicon-rubber stopper. The working electrode was a conventional DME; in most cases, the rate of flow of mercury was 0.526 mg s^{-1}, and the drop-time was mechanically controlled at 4.1 s. Admittance measurements were made on a surface area of 0.0142 cm^2. A platinized-platinum spiral of large surface area was used as a counter electrode. The reference electrode was a silver-silver chloride electrode placed in the cell as shown in Fig. 1; this location of the reference electrode is not desirable from the standpoint of eliminating the ohmic *IR*-drop, but is essential for the stable performance of the potentiostat when a high-impedance system is to be measured. The correction of the electrode potential for the ohmic drop was made by calculating the *IR*-values assuming an appropriate value of the solution resistance.

The measurements were made with deaerated solutions at 25.0$\pm$0.1 °C. All solutions were prepared from analytical reagent grade chemicals and redistilled water.

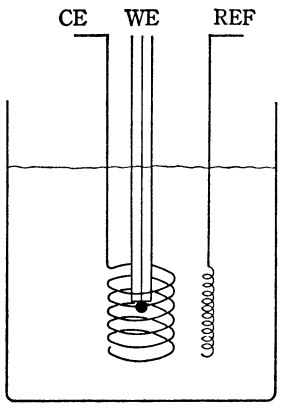

Fig. 1. Position of the electrodes; WE, dropping mercury electrode; CE, platinized-platinum counter electrode; REF, Ag-AgCl reference electrode.

Results and Discussion

Frequency Dependence of the Electrode Impedance and a Possible Equivalent Circuit. A typical DC-polarogram of a DME/1 mM KCl system is presented in Fig. 2; the potential regions F_1, P, and F_2 correspond to the reduction wave of K^+, the limiting current plateau, and the reduction of water, respectively. In this paper, the impedance behavior in the potential region P ($E=-2.7$ to -0.3 V *vs.* Ag–AgCl) will be discussed.

Figure 3 shows the potential dependence of the series capacitance C_s and the series resistance R_s of the impedance observed with a DME/1 mM KCl system at several frequencies. A remarkable frequency dispersion of C_s and R_s is observed at each electrode potential of the cathodic limiting current plateau. The value of C_s is clearly lower than that of the conventional double layer (about 16 μF cm^{-2}), and R_s is much higher than that corresponding to the resistance of the bulk solution.

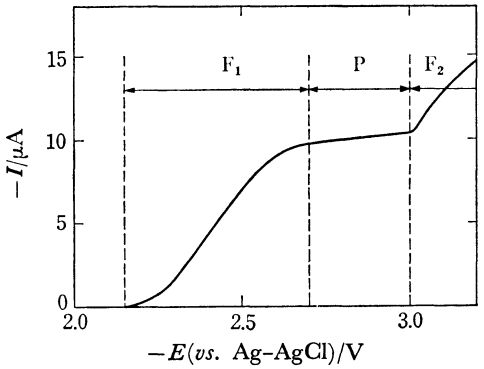

Fig. 2. Current-potential curve obtained with a DME/1 mM KCl system at 25 °C: F_1, the potential region of the reduction step of K^+; P, the limiting current plateau; F_2, the potential region of the reduction of water.

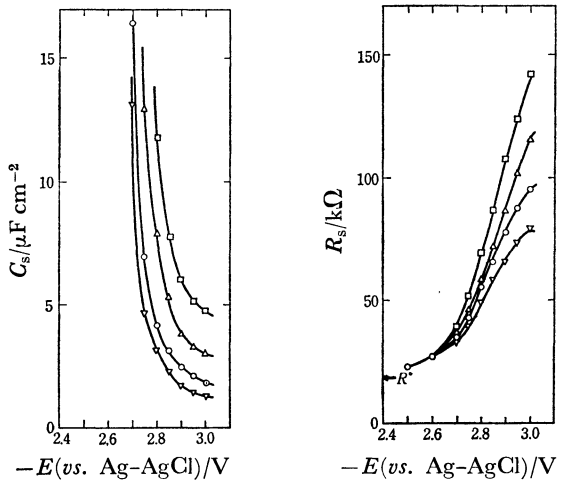

Fig. 3. Potential dependence of the series capacitance C_s and resistance R_s of a DME/1 mM KCl system (25 °C) at different frequencies: -□- 32 Hz, -△- 64 Hz, -○- 120 Hz, -▽- 250 Hz. R° is the resistance of solution as defined by Eq. (12).

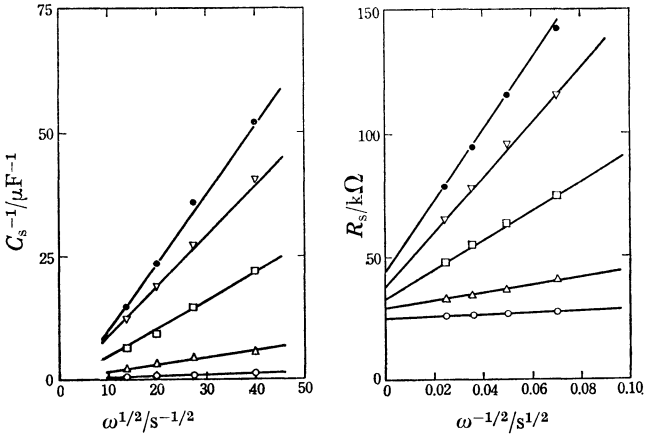

Fig. 4. Frequency dependence of the C_s- and R_s-components of a DME/1 mM KCl system (25 °C) at various electrode potentials: E(*vs.* Ag-AgCl)/V= -2.6(-○-), -2.7(-△-), -2.8(-□-), -2.9(-▽-), and -3.0(-●-).

Table 1. The intercepts and the slopes of Eqs. (1) and (2), obtained with a DME/1 mM KCl system at 25.0 °C

$-E$ (*vs.* Ag-AgCl)/V	$(C_s^\circ)^{-1}$ / μF^{-1}	S_c / Ω s$^{-1/2}$	R_s° / kΩ	S_r / Ω s$^{-1/2}$
2.6	~0	3.5×10^4	25	4.0×10^4
2.7	~0	1.4×10^5	29	1.6×10^5
2.8	−1	5.7×10^5	33	6.0×10^5
2.9	−1	1.04×10^6	38	1.12×10^6
3.0	−4	1.41×10^6	44	1.46×10^6

In Fig. 4, the C_s and R_s at each electrode potential are plotted as a function of the angular frequency ω. From the linear relationship observed with the C_s^{-1} *vs.* $\omega^{1/2}$ and the R_s *vs.* $\omega^{-1/2}$ plots, the frequency dependence of C_s and R_s can be represented by the following equations:

$$C_s^{-1} = (C_s^\circ)^{-1} + S_c\omega^{1/2} \quad (1)$$

$$R_s = R_s^\circ + S_r\omega^{-1/2} \quad (2)$$

The intercepts ($(C_s^\circ)^{-1}$ and R_s°) and the slopes (S_c and S_r) as given by Eqs. (1) and (2) are summarized in Table 1. It can be assumed from this result that, at each potential, $S_c=S_r=S$ and $(C_s^\circ)^{-1}=0$ within the limit of experimental accuracy. With this approximation, Eqs. (1) and (2) can be reduced to

$$C_s^{-1} = S\omega^{1/2} \quad (3)$$

$$R_s = R_s^\circ + S\omega^{-1/2} \quad (4)$$

Figure 5(a) shows the simplest electrical equivalent circuit which satisfies the impedance behavior represented by Eqs. (3) and (4). The impedance Z_w is a Warburg-type impedance given by

$$Z_w = R_w + jX_w \quad (5)$$

with

$$R_w = -X_w = S\omega^{-1/2} \quad (6)$$

The magnitude of Z_w is equal to $\sqrt{2}S\omega^{-1/2}$, and the phase angle between R_w and X_w is equal to $\pi/4$.

Consider a simple electrode reaction,

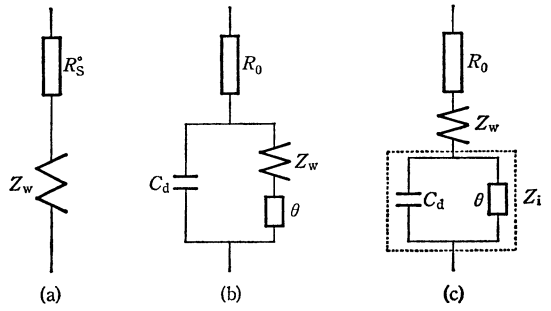

Fig. 5. Electrical equivalent circuits of the electrode impedance.

$$M^+ + e(Hg) \rightleftharpoons M\text{-}Hg \quad (M: \text{alkali-metal}) \qquad (7)$$

in which the mass-transport of M^+ and M in mercury is controlled by diffusion. According to the theory of electrode processes,[11,12] the equivalent circuit for the electrode reaction (7) in solutions containing an excess of supporting electrolytes is represented by Fig. 5(b), where C_d is the conventional double-layer capacitance; θ, the polarization resistance; and R_0, the resistance of solution. This equivalent circuit implicitly involves the assumption that different kinds of ions are responsible for the faradaic and the double-layer charging processes, *i.e.*, the faradaic process is controlled by the depolarizer flux, while the charging process is controlled by the supporting electrolyte flux.

In solutions containing no supporting electrolytes, however, both the faradaic and charging processes may be controlled by the flux of the same ionic species—alkali-metal cations, in the present systems. When alkali-metal cations reach the electrode surface by mass-transport, they will contribute to both faradaic and charging currents. In such cases, the equivalent circuit is considered to be represented by Fig. 5(c), where the Warburg impedance of the depolarizer is in series with the impedance of electrode interface, Z_i, which involves θ and C_d. If the flux of the depolarizer contributes mainly to the charging process, the impedance Z_i should be capacitive, while, if the flux contributes mainly to the faradaic process, Z_i should be resistive.

The equivalent circuit (Fig. 5(a)) determined by the impedance measurements shows that the impedance Z_i in Fig. 5(c) should be resistive, *i.e.*, the condition

$$\theta \ll 1/\omega C_d \qquad (8)$$

is satisfied at the frequencies used in the present study. This relationship is reasonable, because the electrode reaction (7) is known to be polarographically reversible and the polarization resistance θ is very small. In this case, the Warburg-type impedance in Fig. 5(a) can be considered to be due to the mass-transport of the depolarizer, and the resistance R_s° is assumed to be practically equal to the resistance, R_0, of the solution.

Resistance Component R_s°. It should be mentioned that the resistance component R_s° observed with the DME/KCl system depends on the electrode potential as shown in Fig. 6. Such a potential-dependence

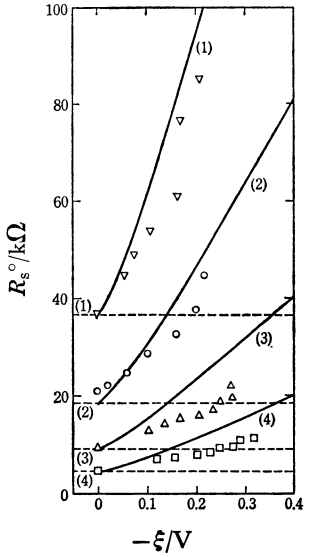

Fig. 6. Potential dependence of resistance R_s° of a DME/x mM KCl system (25 °C): x=0.5(1, ▽), 1.0 (2, ○), 2.0(3, △), and 4.0(4, □). Solid lines are theoretical curves, and broken lines represent the R°-values for each concentration. Potential axis $\xi = E_{cor} - E_{1/2}{}^r$ (see text).

of R_s° can be explained by taking into account the contribution from the resistance R_m of a mass-transport layer where the concentration of depolarizer changes with the distance from the electrode surface. The resistance component R_s° is then given by

$$R_s^\circ \simeq R_o = R_m + R_b \qquad (9)$$

R_b being the resistance of the bulk solution where the composition of the solution is uniform.

In the present systems containing no supporting electrolytes, the resistance R_m is expected to increase with an increase in the negative electrode potential because of the decrease in the concentration of depolarizer at the electrode surface. In the following calculation, we assume that the concentration change of the depolarizer is linear in the mass-transport layer (the Nernst-type layer) as shown in Fig. 7 and that the ionic mobilities are constant throughout the solution phase.

With these approximations, the resistance of the mass-transport layer R_m and that of the bulk solution R_b are given by the following equations:

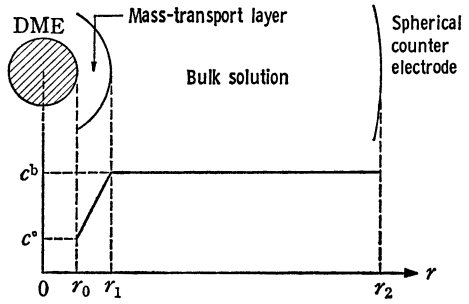

Fig. 7. A model of the mass-transport layer.

$$R_m = R^\circ c_M^b\left(\frac{1}{r_0}-\frac{1}{r_2}\right)^{-1}\frac{r_1-r_0}{r_1c_M^\circ-r_0c_b^M} \times\left[\left(\frac{1}{r_0}-\frac{1}{r_1}\right)+\frac{c_M^b-c_M^\circ}{r_1c_M^\circ-r_0c_M^b}\ln\frac{r_0c_M^b}{r_1c_M^\circ}\right] \quad (10)$$

and

$$R_b = R^\circ\left(\frac{1}{r_0}-\frac{1}{r_2}\right)^{-1}\left(\frac{1}{r_1}-\frac{1}{r_2}\right) \quad (11)$$

with

$$R^\circ = \frac{1000}{4\pi\Lambda c_M^b}\left(\frac{1}{r_0}-\frac{1}{r_2}\right) \quad (12)$$

where c_M^b and c_M° are the concentrations of M^+ in the bulk solution ($r_1 \leq r \leq r_2$) and at the electrode surface ($r=r_0$), respectively, and Λ is the molar conductivity of the solution. The value of R° corresponds to the resistance of the solution phase when the composition of the solution is uniform from r_0 to r_2; R° can be determined from the measurement at potentials where no electrode reaction occurs.

In the calculation of R_s° using Eqs. (9)—(12) as a function of the electrode potential, the following two assumptions are introduced:

$$\delta = r_1 - r_0 = \left(\frac{3}{7}\pi D_M t\right)^{1/2} \quad (13)$$

and

$$\frac{c_M^b-c_M^\circ}{c_M^\circ} = \exp\left(\frac{-F}{RT}\xi\right) \quad (14)$$

with

$$\xi = E_{cor} - E_{1/2}{}^r \quad (15)$$

where δ is the thickness of the mass-transport layer, D_M the diffusion coefficient of the depolarizer M^+, t the time of electrolysis, $E_{1/2}{}^r$ the reversible half-wave potential, and E_{cor} the electrode potential corrected for the ohmic IR-drop. Relation (13) is obtained from the theory of the polarographic limiting current, and relation (14) is based upon the Nernstian behavior of the electrode reaction.[13]

In Fig. 6, the experimental relationship between R_s° and ξ is compared with the theoretical curves (solid lines) obtained with the numerical values: $r_0=0.0339$ cm, $r_2=0.5$ cm, $t=4.0$ s, and $D_M=1\times10^{-5}$ cm^2 s^{-1}. The agreement between the experimental and the theoretical curve is sufficiently good to support the assumption that R_s° is the resistance of the solution phase from r_0 to r_2 as represented by the simplified model shown in Fig. 7.

Warburg-type Impedance Z_w. Let us assume that the Warburg-type impedance in our present system is given by an expression[12] similar to that derived for the electrode reaction in the supporting electrolyte solutions. Then, the coefficient σ of the Warburg impedance for electrode reaction (7) may be given by the equation,

$$\sigma = SA = \frac{RT}{\sqrt{2}F^2}\left[\frac{1}{\sqrt{D_A^*}}\exp\left(\frac{\alpha_aF}{RT}\xi\right)+\frac{1}{\sqrt{D_M^*}}\times\exp\left(-\frac{\alpha_cF}{RT}\xi\right)\right]\left[\alpha_ac_a^\circ\exp\left(\frac{\alpha_aF}{RT}\xi\right)+\alpha_cc_M^\circ\exp\left(-\frac{\alpha_cF}{RT}\xi\right)\right]^{-1} \quad (16)$$

where A is the surface area of the electrode, $\alpha_{a(c)}$ the anodic (cathodic) transfer coefficient, $D_{a(M)}^*$ the apparent diffusion coefficient of M-Hg (M^+), $c_{a(M)}^\circ$ the concentration of M-Hg (M^+) at the electrode surface, and other symbols have their usual meanings.

At sufficiently negative potentials where the cathodic limiting current is observed, the following conditions can be satisfied:

$$c_a^\circ \simeq c_M^b \quad (17)$$

and

$$\exp\left(\frac{\alpha_aF}{RT}\xi\right) \ll \exp\left(-\frac{\alpha_cF}{RT}\xi\right) \quad (18)$$

Then, assuming the relation, $\alpha_a+\alpha_c=1$, we obtain the expression:

$$\sigma = \frac{RT}{(2D_M^*)^{1/2}F^2}\left[\alpha_ac_M^b\exp\left(\frac{F}{RT}\xi\right)+\alpha_cc_M^\circ\right]^{-1} \quad (19)$$

Equation (19) shows that the experimental values of σ provide information on the surface concentration c_M° of the depolarizer at each potential ξ. If the surface concentration is determined by the Nernstian relation, expression (20) can be obtained from Eqs. (14) and (19):

$$\sigma = \frac{RT}{(2D_M^*)^{1/2}F^2c_M^b}\exp\left(-\frac{F}{RT}\xi\right) \quad (20)$$

In Fig. 8, the experimental values of σc_M^b obtained with several alkali-metal chlorides are plotted against the electrode potential ξ; the theoretical line with the slope given by Eq. (20) is also shown. Considering the accuracy of the measurements and the rough approximations involved in the theoretical calculation, we can conclude that the agreement between the

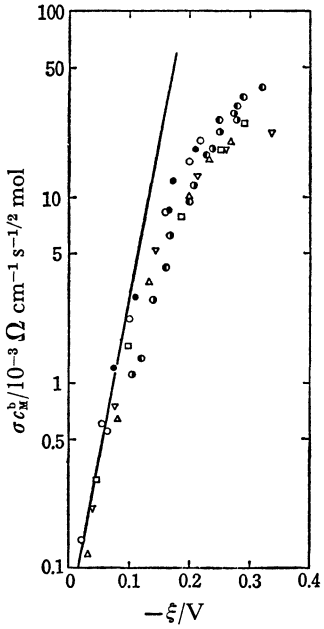

Fig. 8. Potential dependence of the Warburg-parameter σc_M^b of DME/alkali-metal chloride systems (25 °C): 0.5 mM KCl(-●-); 1.0 mM KCl(-○-); 2.0 mM KCl(-◑-); 4.0 mM KCl(-◐-); 1.0 mM NaCl (-□-); 1.0 mM RbCl(-△-); 1.0 mM CsCl(-▽-). Solid line shows the theoretical curve as calculated with $D_M^*=1\times10^{-5}$ cm^2 s^{-1} by means of Eq. (20).

experiments and the theory is satisfactory unless $|\xi|$ exceeds 150 mV.

Conclusion

The present results show that the impedance behavior of the DME/MCl (M: alkali-metal) system at the potentials of the limiting current plateau (region P in Fig. 2) can be represented by the equivalent circuit as shown in Fig. 5(a); the Warburg impedance Z_w for electrode reaction (7) is in series with resistance R_s° of the solution from the surface of the working electrode to the counter electrode. It is interesting that, at relatively low frequencies ($\leq$250 Hz), the impedance in the potential region P behaves as if the conventional double-layer were absent. For this situation, the interfacial layer between the electrode and the solution phase may be called "the Nernst double-layer"; the potential difference across the Nernst double-layer is determined by the electrode reaction, and the formation of the layer is controlled by the mass-transport of the reacting species.

References

1) D. C. Grahame, *Chem. Rev.*, **41**, 441 (1947).
2) M. J. Sparnaay, "The Electrical Double Layer," The International Encyclopedia of Physical Chemistry and Chemical Physics 4/14, Pergamon Press, Oxford (1972).
3) P. Delahay, R. de Levie, and A. M. Giuliani, *Electrochim. Acta*, **11**, 1141 (1966).
4) R. D. Armstrong and W. P. Race, *J. Electroanal. Chem.*, **33**, 285 (1971).
5) F. C. Anson, R. F. Martin, and C. Yarintzky, *J. Phys. Chem.*, **73**, 1835 (1969).
6) K. Takahashi and R. Tamamushi, *Electrochim. Acta*, **16**, 875 (1971).
7) K. Takahashi and R. Tamamushi, *ibid.*, **16**, 1157 (1971).
8) M. Sluyters-Rehbach and J. H. Sluyters, *J. Electroanal. Chem.*, **34**, 55, 69 (1972); **36**, 101, 287 (1972).
10) K. Matsuda, K. Takahashi, and R. Tamamushi, *Sci. Papers Inst. Phys. Chem. Res.*, **64**, 62 (1970).
11) P. Delahay, "New Instrumental Methods in Electrochemistry," Chap. 7, Interscience Publishers, Inc., New York (1954).
12) M. Sluyters-Rehbach and J. H. Sluyters, "Electroanalytical Chemistry", Vol. 4 (Allen J. Bard, ed.), Marcel Dekker, Inc., New York (1970), pp. 16—18.
13) See for example: G. W. C. Milner, "The Principles and Applications of Polarography and other Electroanalytical Processes", Chap. 3 and 4, Longmans, Green and Co., London (1957).